

Average exit time for volume-preserving maps

J. D. Meiss

Program in Applied Mathematics, University of Colorado, Boulder, Colorado 80304

(Received 15 April 1996; accepted for publication 24 June 1996)

For a volume-preserving map, we show that the exit time averaged over the entry set of a region is given by the ratio of the measure of the accessible subset of the region to that of the entry set. This result is primarily of interest to show two things: First, it gives a simple bound on the algebraic decay exponent of the survival probability. Second, it gives a tool for computing the measure of the accessible set. We use this to compute the measure of the bounded orbits for the Hénon quadratic map. © 1997 American Institute of Physics. [S1054-1500(97)00101-8]

One important aspect of chaos in conservative dynamical systems is that chaotic and regular regions are inter-mixed in an intricate way in the phase space. This can have important implications for transport properties of these systems. For example, orbits of an area-preserving map are eternally trapped in a region if they are enclosed by an invariant circle, but can leak through destroyed circles (cantori). In this paper we obtain an effective technique for computing the fraction of trapped orbits. The result, applied to the Hénon map, shows that the trapped fraction depends in an intricate way on the structure of the chaotic set.

I. INTRODUCTION

In this paper we study the time of escape for orbits that begin in a specified region A under the dynamics of a map f on a phase space M . We discuss the *exit time*, the time for a point to first exit the set, and the *transit time*, the time for a point to traverse the set. The *exit time distribution* is the probability distribution of exit times. Our primary goal is to use this distribution to probe the trapped invariant set. The trapped set is generally quite difficult to compute, and is of interest because its boundaries are extremely “sticky”¹⁻¹³ and so even untrapped orbits feel its influence. Our results apply to volume-preserving maps in any dimension where the mechanisms for trapping and escape are much less understood.¹⁴

The theoretical result obtained in this paper is not new—it was essentially obtained by Kac in 1947,^{15,16} and he even quotes earlier results of Birkhoff (1931) and Smoluchowski (1916). Kac was studying the mean first return time to a region in a bounded phase space for an ergodic system; this can be called the mean Poincaré recurrence time or Poincaré cycle. He obtains his result as a consequence of the Poincaré recurrence theorem.¹⁶ We reformulate the result for nonergodic systems, and show how it can also be obtained by considering the mean first exit time.

In his 1957 lecture Kac¹⁶ remarks that the mean recurrence time is “the only quantity which is tractable for general dynamical systems;” however, he abandons it as “relatively useless.” We will not take this admonition to heart,

and use our formulation to compute the measure of the trapped orbits.

As an example, consider Hénon’s area-preserving, quadratic map, which we write as

$$H:(x,y) \rightarrow (y - k + x^2, -x). \quad (1)$$

We are interested in the set of bounded orbits. It is possible to show that (for $k > -1$) all bounded orbits are contained in the square $\{z = (x, y) : |x, y| < x_s\}$ where $x_{s,e} = 1 \pm \sqrt{1+k}$. Here we denote the two fixed points (for $k > -1$) by $z_e = (x_e, -x_e)$ and $z_s = (x_s, -x_s)$. The first is elliptic when $-1 < k < 3$, and the second is a saddle. Bounded orbits include all periodic orbits and all orbits within invariant circles; for example, the latter exist in the neighborhood of z_e providing it is elliptic and has a rotation number, ω , that is not $\frac{1}{3}$ or $\frac{1}{2}$ (i.e., $k \neq \frac{5}{4}$ or ≥ 3). Hyperbolic orbits can also be trapped: for example, those that are homoclinic to the saddle fixed point.

In his original paper,¹⁷ Hénon studied the set of bounded orbits of H (in a different coordinate system than ours) by iterating points along a segment of the symmetry line ($x = -y$) to determine the subintervals that did not reach a fixed large distance from the origin within 100 iterations. He noted that as k varies, the boundaries of the trapped intervals either closely follow the position of an unstable rotational periodic point or else an island around an elliptic periodic point. Channon and Leibowitz¹⁸ studied the escape and trapping from the period 5 island chain in the Hénon map at $k = -0.422$. They identified the exit and entrance lobes of the resonance as the important sets to consider. Studying the fifth power of the map, they started 7750 orbits in the outer entrance lobe and computed the survival probability distribution. This was found to decay as $t^{-\alpha}$ with $\alpha = 0.5$ for short times (up to 10 iterates), but deviated from this for moderate times (up to 45 iterates).

Karney¹⁹ also considered the Hénon map, and studied the survival probability for a square A enclosing all bounded orbits. He mostly studied $k = -0.6$ where the most prominent island chain is period 6. Karney’s primary object of study was the “trapping time statistic” which is proportional to the exit time distribution for A . He found that this distribution decayed as $t^{-(\alpha+2)}$ with α about 0.25, for times up to 10^4 iterates, though the slope subsequently appears to vary for times up to 10^8 . Chirikov and Shepelyansky²⁰ computed the Poincaré recurrence distribution for the standard map when

there is a critical golden circle, obtaining $\alpha=0.34$ up to 10^5 iterates. Though algebraic decay has been observed in many Hamiltonian systems and symplectic maps (indeed, whenever there are elliptic orbits the decay appears to be algebraic), the exponent for the decay is apparently not universal.²¹ One reason this might be so, according to Murray,²² is that the self-similar limit is not reached for ‘‘short’’ time computations. The Poincaré recurrence distribution has also been computed for flows, for example by Zaslavsky and Tippet.²³ [Interestingly, they speculate that a relation like our Eq. (13) holds.]

Rom-Kedar and Wiggins have emphasized the fact that one can obtain a complete description of transport through a region by considering the future history of only the entering trajectories.⁵ Using their notion of ‘‘lobe dynamics’’ for a homoclinic tangle, they obtained an expression for the accessible region in terms of the exit time distribution—we will use a slightly generalized version of this below.

II. DEFINITIONS

Let $f:M \rightarrow M$ be a homeomorphism with an invariant measure μ . For measurable sets $A, B \subset M$, the *crossing time* (or first passage time) for $a \in A$ to B is defined as

$$t_{A \rightarrow B}(a) = \min_{n > 0} (n : f^n(a) \in B). \tag{2}$$

We let $t_{A \rightarrow B}(a) = \infty$ if a never reaches B . If B is the complement of A , then the crossing time is called the (forward) *exit time*

$$t^+(a) = t_{A \rightarrow M \setminus A}(a). \tag{3}$$

Similarly the backward exit time for $a \in A$ is defined as

$$t^-(a) = \min_{n > 0} (n : f^{-n}(a) \notin A). \tag{4}$$

If $B = A$, then the crossing time is called the first return time:

$$t_{\text{return}}(a) \equiv t_{A \rightarrow A}(a), \quad \text{for } a \in A. \tag{5}$$

According to our definition $t_{\text{return}}(a) \geq 1$, and is equal to 1 whenever the point does not leave on the first iterate. We define the *exit set* $E \subset A$ as the subset with exit time 1, and the *entry* (or incoming) *set* $I \subset A$ as the set with backward exit time 1; equivalently,

$$E = A \setminus f^{-1}(A), \quad I = A \setminus f(A). \tag{6}$$

The *turnstile* is the union of E and I .

As an example, consider the Hénon map in Eq. (1). A natural choice for the region A is the ‘‘resonance zone,’’ shown in Fig. 1, consisting of the region bounded by the segments of the left-going branches of the stable and unstable manifolds of the saddle fixed point up to their first intersection on the symmetry line ($x = -y$). This region contains all bounded orbits of H .

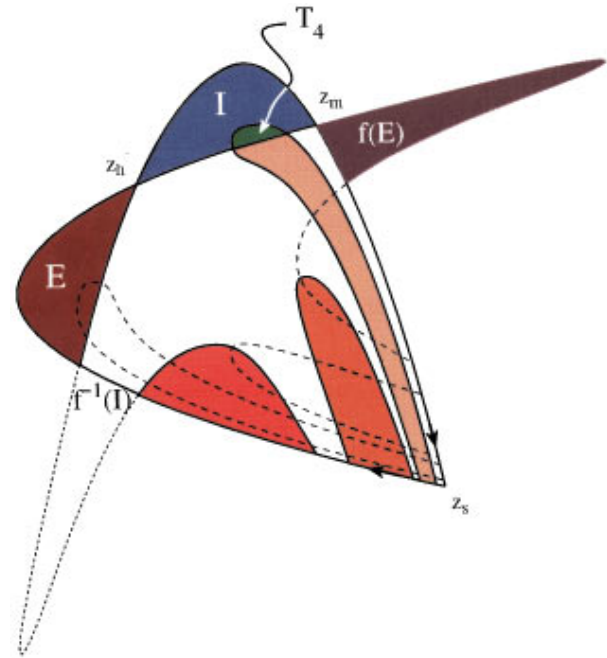


FIG. 1. Exit and entry sets for the fixed point resonance of the Hénon map for $k=0.5$.

The transit time of a point a is the sum of its forward and backward exit times minus 1 (to get rid of an annoying term),

$$t_{\text{transit}}(a) \equiv t^+(a) + t^-(a) - 1. \tag{7}$$

The transit time is an orbit invariant: each point along an orbit has the same transit time. The *transit time decomposition* of a set is the partition of a set into subsets with equal transit time. We denote the transit time decomposition of the entry set I by sets T_j ; this is also the part of I with exit time j :

$$T_j = \{a \in I : t^+(a) = j\}. \tag{8}$$

For example, we show the first few preimages of the exit set in sequentially lighter shades of red for the Hénon resonance zone in Fig. 1. For this parameter value $T_1 = T_2 = T_3 = \emptyset$ and T_4 is shown. A partial transit time decomposition of the Hénon entry set is shown in Fig. 2.

By measure preservation, almost every point that enters A must eventually escape, so

$$\mu(E) = \mu(I) = \sum_{j=1}^{\infty} \mu(T_j). \tag{9}$$

The accessible set, $A_{\text{acc}} \subset A$ is defined to be the set with finite backward exit time; it is the set that can be reached from the outside:

$$A_{\text{acc}} = \{a \in A : t^-(a) < \infty\}. \tag{10}$$

Of course, the set with finite exit time differs from A_{acc} at most by a set of measure zero, since the set that enters but never exits must have measure zero.

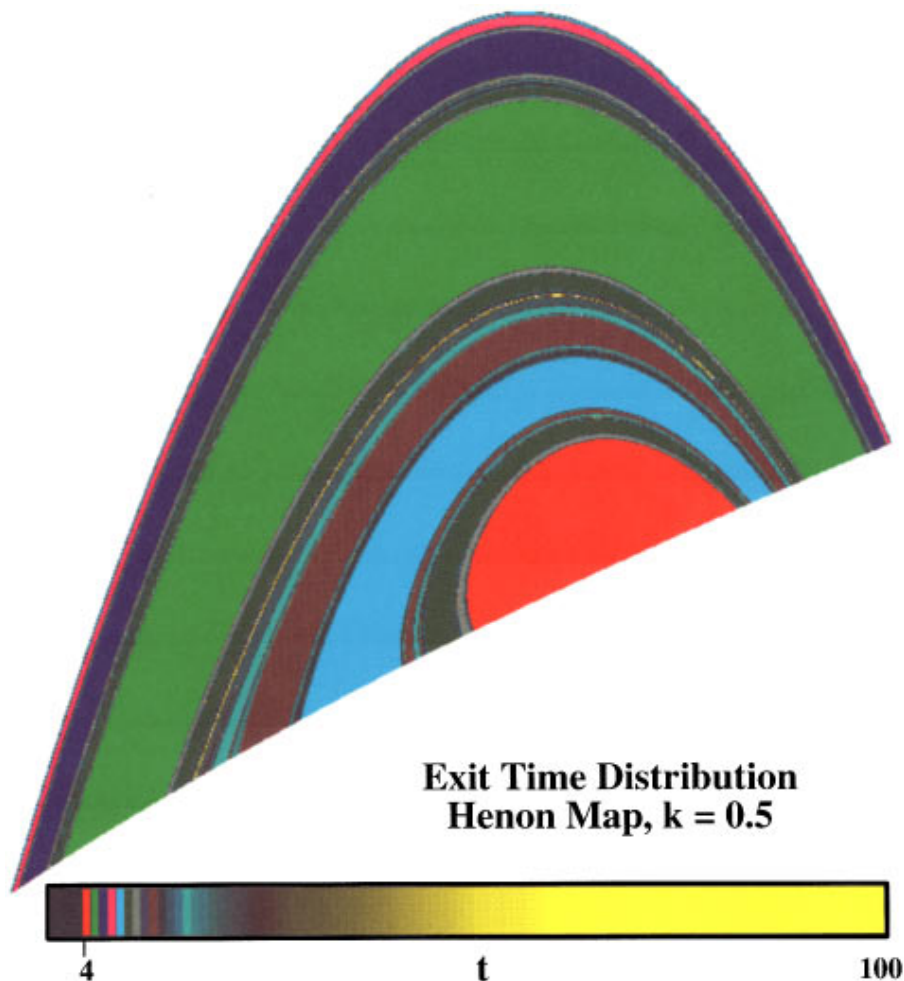


FIG. 2. Exit time decomposition of the entry set of the Hénon trellis at $k=0.5$. Color scale is given at the bottom.

III. AVERAGE EXIT TIME

In this paper we are interested in these transport times averaged over sets of initial conditions. For a function $g(z)$ we denote

$$\langle g \rangle_S \equiv \frac{1}{\mu(S)} \int_S g(z) d\mu.$$

Remarkably, there are some simple formulas for average transport times. The following lemma was stated for volume preserving flows (without its elementary proof) in Ref. 24 and is implicitly obtained for two-dimensional maps in Ref. 25.

Average Exit Time Lemma: The average exit (transit) time for incoming orbits is

$$\langle t^+ \rangle_I = \langle t_{\text{transit}} \rangle_I = \frac{\mu(A_{\text{acc}})}{\mu(I)}. \tag{11}$$

Proof: Since $T_j \subset I$ are disjoint and cover almost all of I and the exit (and transit) time of the set T_j is j , the average exit time is given by

$$\langle t^+ \rangle_I = \frac{1}{\mu(I)} \sum_{j=1}^{\infty} j \mu(T_j),$$

assuming the sum exists. Given the transit time decomposition T_j , we can compute the accessible subset of A using the sets

$$T_j^i = f^i(T_j).$$

Note that $T_j^i \subset A$ for $i=0, \dots, j-1$, and that these sets are disjoint because they have transit time j and backward exit time $i+1$. Furthermore the union of these sets is, up to measure zero, the entire subset of A that exits. Thus by definition

$$A_{\text{acc}} = \bigcup_{j=1}^{\infty} \bigcup_{i=0}^{j-1} T_j^i \Rightarrow \mu(A_{\text{acc}}) = \sum_{j=1}^{\infty} \sum_{i=0}^{j-1} \mu(T_j^i).$$

Since measure is preserved $\mu(T_j^i) = \mu(T_j)$, and so

$$\mu(A_{\text{acc}}) = \sum_{j=1}^{\infty} j \mu(T_j). \tag{12}$$

An almost identical expression was obtained by Kac (see Ref. 16, p. 66) though he does not make the interpretation about the accessible region. Rom-Kedar and Wiggins have also obtained this result.²⁵ Comparing Eq. (12) with the expression for $\langle t^+ \rangle_I$ gives the lemma. Finally since $\mu(A_{\text{acc}}) \leq \mu(A)$, it is clear that the sum in Eq. (12) converges. \square

Since $\mu(A_{\text{acc}})$ is finite, a simple consequence of this result is:

Corollary 1: The measure of the region with transit time t must decay faster than t^{-2} .

Furthermore, the lemma implies well-known results for the average return time obtained by Kac and Smoluchowski (Refs. 15–16). In our context these can be generalized to:

Corollary 2 (Smoluchowski): Suppose $\mu(M)=1$. The average first return time for points that escape in one step from $A \subset M$ is

$$\langle t_{\text{return}} \rangle_E = 1 + \frac{\mu(M_{\text{acc}} \setminus A)}{\mu(E)} = 1 + \frac{\mu(M_{\text{acc}}) - \mu(A)}{\mu(E)},$$

where M_{acc} is the subset of M that is accessible to orbits beginning in A .

Proof: Consider the set $M \setminus A$. Points enter it by escaping from A , so the entry set of $M \setminus A$ is $f(E)$. The corollary follows from the Lemma if we replace A_{acc} by $M_{\text{acc}} \setminus A$, and I by $f(E)$. We then add one to the result, since the return time to A is one larger than the transit time through M . \square

Corollary 3 (Kac): Suppose $\mu(M)=1$. The average first return time to a region $A \subset M$ is

$$\langle t_{\text{return}} \rangle_A = \frac{\mu(M_{\text{acc}})}{\mu(A)}, \tag{13}$$

where M_{acc} is the subset of M that is accessible to orbits beginning in A .

Proof: For points that stay in A for at least one step, the first return time is one. The remaining portion of A is its exit set E . We use Corollary 2 for the return time for these points. So the average first return time to A is

$$\langle t_{\text{return}} \rangle_A = \frac{1}{\mu(A)} [(\mu(A) - \mu(E)) \times 1 + \mu(E) \times \langle t_{\text{return}} \rangle_E].$$

This reduces to the promised result. \square

We can also easily compute the transit time averaged over A :

Corollary 4: The average transit time for points that do escape from A is

$$\langle t_{\text{transit}} \rangle_{A_{\text{acc}}} = \frac{1}{\mu(A_{\text{acc}})} \sum_{j=1}^{\infty} j^2 \mu(T_j), \tag{14}$$

providing that this sum converges. In this case, the average exit time for A is

$$\langle t^+ \rangle_{A_{\text{acc}}} = \frac{1}{2} (\langle t_{\text{transit}} \rangle_{A_{\text{acc}}} + 1). \tag{15}$$

Proof: Since each image of T_j has the same transit time, the area of A that has transit time j is $j\mu(T_j)$. This gives (14). Equation (15) follows from

$$\begin{aligned} \langle t^+ \rangle_{A_{\text{acc}}} &= \frac{1}{\mu(A_{\text{acc}})} \sum_{j=0}^{\infty} \mu(T_j) \sum_{k=0}^{j-1} (j-k) \\ &= \frac{1}{\mu(A_{\text{acc}})} \sum_{j=0}^{\infty} \frac{j(j+1)}{2} \mu(T_j). \end{aligned} \quad \square$$

In contrast to the exit time averaged over I , we cannot use disjointness to show that (14) converges. In fact as we show by a simple example in Sec. V, these sums need not converge.

IV. EXIT TIME DISTRIBUTIONS

As was emphasized by Rom-Kedar and Wiggins,⁵ if one knows the T_j , one has most of the information one could want about transport through A . Here we recall some definitions of normalized exit and transit time distributions.

The exit time probability distribution for the entry set is the probability that a trajectory in I will have a given exit time:

$$\text{Prob}(t^+(I) = j) = \frac{\mu(T_j)}{\mu(I)}. \tag{16}$$

Similarly the survival probability is the probability that the exit time will be at least k :

$$\text{Prob}(t^+(I) \geq k) = \frac{1}{\mu(I)} \sum_{j=k}^{\infty} \mu(T_j). \tag{17}$$

Note that $\text{Prob}(t^+(I) \geq 1) = 1$ by Eq. (9).

Once we know the T_j , various distributions for A are also known. For example, since $f^j(T_{k+j}) \subset A_{\text{acc}}$ has exit time k (with backward exit time $j+1$), the subset of A_{acc} that has exit time k is given by $\cup_{j=0}^{\infty} f^j(T_{k+j})$. Thus the exit time probability distribution for A_{acc} is

$$\begin{aligned} \text{Prob}(t^+(A_{\text{acc}}) = k) &= \frac{1}{\mu(A_{\text{acc}})} \sum_{j=k}^{\infty} \mu(T_j) \\ &= \frac{1}{\langle t^+ \rangle_I} \text{Prob}(t^+(I) \geq k), \end{aligned}$$

which is the same as the survival distribution for I in Eq. (17), up to normalization. Similarly the subset of A with transit time j is $\cup_{k=0}^{j-1} f^k(T_j)$, thus the transit time probability is

$$\text{Prob}(t_{\text{transit}}(A_{\text{acc}}) = j) = \frac{1}{\mu(A_{\text{acc}})} \sum_{k=0}^{j-1} \mu(T_j) = j \frac{\mu(T_j)}{\mu(A_{\text{acc}})}.$$

Finally the survival time distribution for A is

$$\begin{aligned} \text{Prob}(t^+(A) \geq k) &= \frac{1}{\mu(A_{\text{acc}})} \sum_{j=k}^{\infty} \sum_{m=j}^{\infty} \mu(T_m) \\ &= \frac{1}{\mu(A_{\text{acc}})} \sum_{j=1}^{\infty} j \mu(T_{k+j}). \end{aligned}$$

Note that these equations imply that if, e.g.,

$$\mu(T_k) \sim k^{-(2+\alpha)}, \text{ as } k \rightarrow \infty,$$

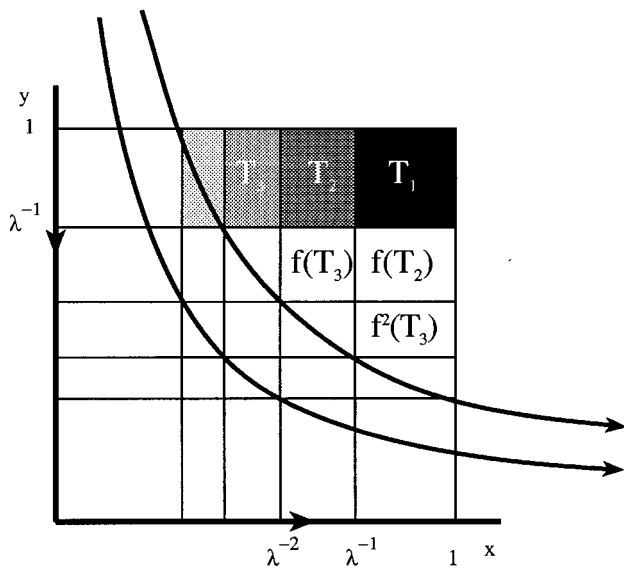


FIG. 3. Transit time decomposition of the entry region for the linear hyperbolic map. The transiting regions T_j , $j=1,2,3$ and a few of their iterates are shown.

where $\alpha > 0$ by Corollary 2, then we have

$$\begin{aligned} \text{Prob}(t^+(I) = k) &\sim k^{-(\alpha+2)}, \\ \text{Prob}(t^+(I) \geq k) &\sim \text{Prob}(t^+(A_{\text{acc}}) = k) \\ &\sim \text{Prob}(t_{\text{transit}}(A_{\text{acc}}) = k) \sim k^{-(\alpha+1)}, \\ \text{Prob}(t^+(A_{\text{acc}}) \geq k) &\sim k^{-\alpha}. \end{aligned}$$

V. EXAMPLES

Consider the linear, area-preserving, hyperbolic map

$$\begin{pmatrix} x' \\ y' \end{pmatrix} = \begin{pmatrix} \lambda & 0 \\ 0 & \lambda^{-1} \end{pmatrix} \begin{pmatrix} x \\ y \end{pmatrix},$$

where $\lambda > 1$. Let A be the unit square $\{(x, y) : 0 \leq x, y \leq 1\}$. Then the entrance set is the rectangle $I = A \setminus f(A) = \{(x, y) : 0 \leq x \leq 1, \lambda^{-1} < y \leq 1\}$. It is easy to see that the transit time decomposition (see Fig. 3) of I is

$$T_j = \{(x, y) : \lambda^{-j} < x \leq \lambda^{1-j}, \lambda^{-1} < y \leq 1\}.$$

So the measures of each of these regions are

$$\mu(T_j) = \frac{(\lambda - 1)(1 - \lambda^{-1})}{\lambda^j}. \tag{18}$$

These decay exponentially, as one would expect. The calculations needed for Eqs. (9), (12), and (14) are derivatives of simple geometric sums, yielding

$$\begin{aligned} \sum_{j=1}^{\infty} \mu(T_j) &= (1 - \lambda^{-1}) = \mu(I), \\ \sum_{j=1}^{\infty} j \mu(T_j) &= 1 = \mu(A), \end{aligned}$$

$$\sum_{j=1}^{\infty} j^2 \mu(T_j) = \frac{\lambda + 1}{\lambda - 1},$$

as required by the lemma. Thus the average transport times are

$$\langle t^+ \rangle_I = \frac{\lambda}{\lambda - 1}, \quad \langle t_{\text{transit}} \rangle_A = \frac{\lambda + 1}{\lambda - 1}, \quad \langle t^+ \rangle_A = \frac{\lambda}{\lambda - 1}. \tag{19}$$

These results are unchanged if we scale the size of A (since the map is linear), or if we replace A by a square centered on the fixed point (since the map is symmetric).

More generally, suppose the map is a diagonal hyperbolic matrix with eigenvalues $(\lambda_1, \lambda_2, \dots, \lambda_d, \mu_{d+1}, \mu_2, \dots, \mu_n)$, where the $\lambda_i > 1$ and the $\mu_j < 1$. Then the entry set of the unit hypercube A is the union of rectangular cylinders:

$$I = \bigcup_{k=d+1}^n \{(x_1, \dots, x_n) \in A : \mu_k < x_k \leq 1\}.$$

If we define $\Lambda = \prod_{i=1}^d \lambda_i$, and $\Pi = \prod_{i=d+1}^n \mu_i$ to be the total expansion and contraction, respectively, then a simple calculation gives the measure of the transit regions by

$$\mu(T_j) = \frac{(\Lambda - 1)(1 - \Pi)}{\Lambda^j}, \tag{20}$$

in complete accord with Eq. (18). In the volume preserving case, we see that $\Lambda \Pi = 1$, and so the formulas Eqs. (9), (12), and (14) again hold, and the average times are given by Eq. (19) with λ replaced by Λ .

A similar formula would apply to the uniform horseshoe. This case, and that of other trellis types, have been treated by Rom-Kedar,²⁵ who estimates the accessible area under the assumption that the transit decomposition stretches uniformly.

Though the region A that we considered above is special, a theorem of Easton¹² implies that the rate of escape for any isolating neighborhoods of an invariant set are asymptotically similar. Thus any region surrounding the fixed point will have escape that is exponential with rate Λ . Similarly, any diagonalizable hyperbolic map with expansion Λ will also have the same asymptotic rate.

Of course, we expect exponential decay of the transit time decomposition for a hyperbolic system. As we remarked in the Introduction, numerical observations of transport, however, indicate that the transit time decomposition decays algebraically when there are elliptic regions in A . The simplest example of this behavior is the trivial shear (see Fig. 4):

$$\begin{aligned} x' &= x + y', \\ y' &= y. \end{aligned}$$

Let A be the unit square as before. Now the entry set is the triangle $I = \{(x, y) : 0 \leq x < y \leq 1\}$. The transit time decomposition is

$$T_j = \{(x, y) \in I : 1 - jy < x < 1 - (j - 1)y\}.$$

These sets have measures that decrease algebraically

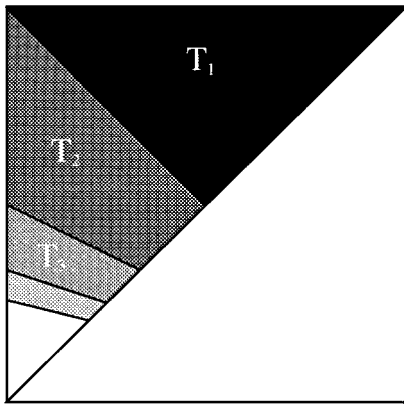


FIG. 4. Transit time decomposition for the simple shear.

$$\mu(T_1) = \frac{1}{4}, \quad \mu(T_j) = \frac{1}{j(j^2 - 1)} \quad j > 1.$$

The sums to get the average transport times are elementary telescoping sums, and again these verify Eqs. (9) and (12). However, for this example the average transit time for A , Eq. (14), does not exist.

VI. BOUNDED ORBITS FOR THE HÉNON MAP

As a final example we use the average transit time, which is straightforward to compute, as an effective method to obtain the accessible area, which is not otherwise computable. Here we do this for the resonance zone of the Hénon map. The calculation involves several steps. First we find the points on the minimizing and maximax homoclinic orbits, z_m and z_h , that bound the lobe (see Fig. 1). We then construct the boundary of the entry set, by discretizing W^u and W^s , as graphs $y^u(x)$ and $y^s(x)$, to a resolution $h = (x_m - x_h)/N$ for a fixed number of pixels N . Generally, in our calculation we used $N = 10^4$. By reversibility, the exit set is the reflection of the entrance set about $x + y = 0$. The average exit time, $\langle t^+ \rangle_I$, is given by an integral of the piecewise constant exit time over the entry set. We do this double integral in the most naive way by first integrating $T(x) = \int_{y^u(x)}^{y^s(x)} t^+(x, y) dy$ for fixed x , and then integrating over x using Simpson's rule. To compute $T(x)$, we use bisection to zoom in on the discontinuities of t^+ : first evaluate t^+ on a grid of size h ; if t^+ does not change between two grid points, we assume (possibly incorrectly) that it is constant between. If there is a change, we bisect the interval until either t^+ is equal on the endpoints, or the perceived error in neglecting the variation in t^+ is small enough (we chose an error of 10^{-3} for this). Also, we truncate t^+ at some maximum value, usually $t_{\max} = 10^6$. Then $T(x)$ is the sum of the t^+ values times the interval lengths. The resulting average exit time is shown in Fig. 5. Though $\langle t^+ \rangle_I$ is generally decreasing as a function of k , there are numerous small upward jumps. We discuss these more below.

The area of the lobe is either given by summing the number of pixels in the exit set, or taking the difference in

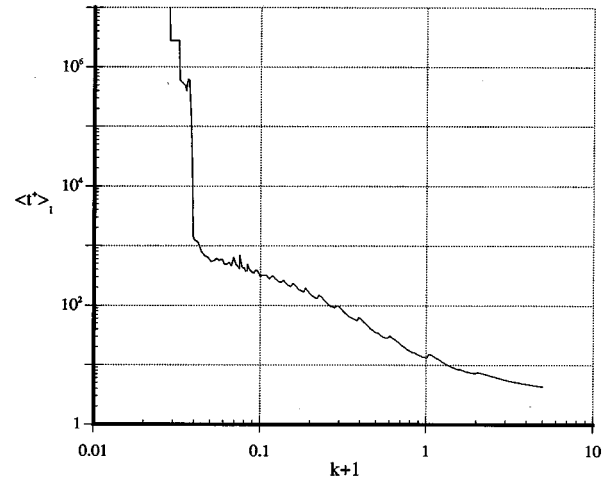


FIG. 5. Average exit time for the Hénon map as a function of parameter. Most points used $N = 10^4$ and $t_{\max} = 10^6$, though for $k < -0.95$, we used $t_{\max} = 5 \times 10^7$.

action between the two homoclinic points.²⁷ Then $\mu(A_{\text{acc}})$ is obtained from Eq. (11). It is interesting to compare this with the total area of the resonance zone itself, $\mu(A)$. This is most easily computed by taking the difference in action between the action of the minimax homoclinic point and the fixed point.²⁷ These areas are shown in Fig. 6.

Note that the resonance and lobe area grow monotonically and smoothly. The value $k = -1$ corresponds to the saddle-node bifurcation, where the fixed point resonance zone is created. Slightly above this point, the lobe area, ΔW

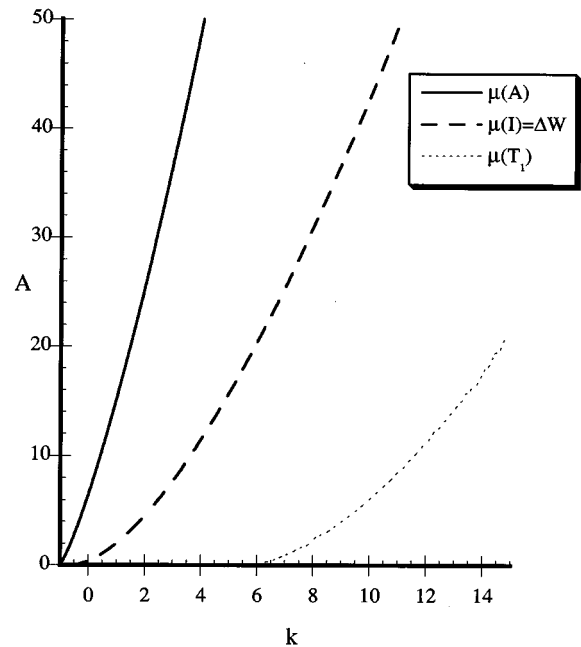


FIG. 6. Resonance and lobe area for the Hénon map. Also shown is $\mu(T_1)$, which is nonzero beyond the formation of the geometric horseshoe at $k \approx 5.706$.

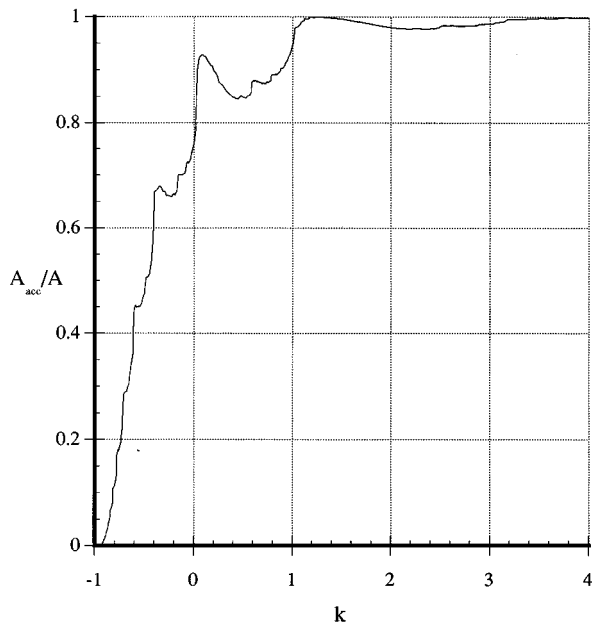


FIG. 7. Accessible fraction for the fixed point resonance of the Hénon map.

is exponentially small²⁸ and most of the resonance is filled with invariant curves.

Combining these results, using Eq. (11) gives the accessible area. In Fig. 7 we show the accessible fraction, $\mu(A_{acc})/\mu(A)$. The area that is inaccessible, which is identical to the measure of the bounded orbits is given by

$$\mu(A_i) = \mu(A) - \mu(A_{acc}) = \mu(A) - \mu(I)\langle t^+ \rangle_I.$$

This area is shown in Fig. 8; this figure is nearly identical to Fig. 4 of Ref. 1, but our method allows us to compute the results to much higher precision. The accuracy can be seen

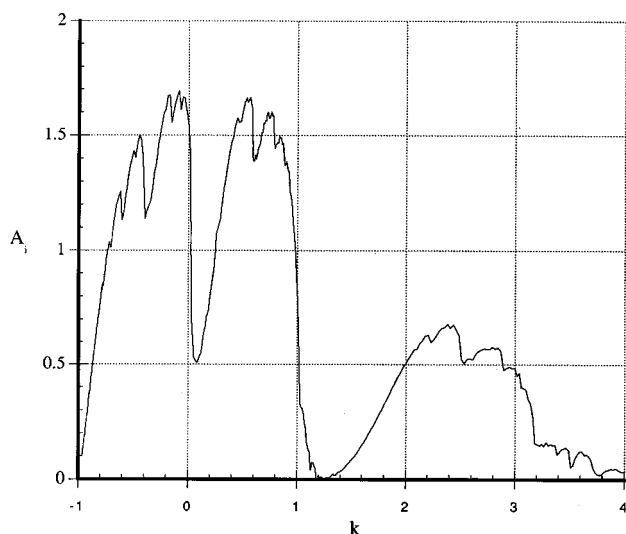


FIG. 8. Measure of the bounded orbits for the Hénon map.

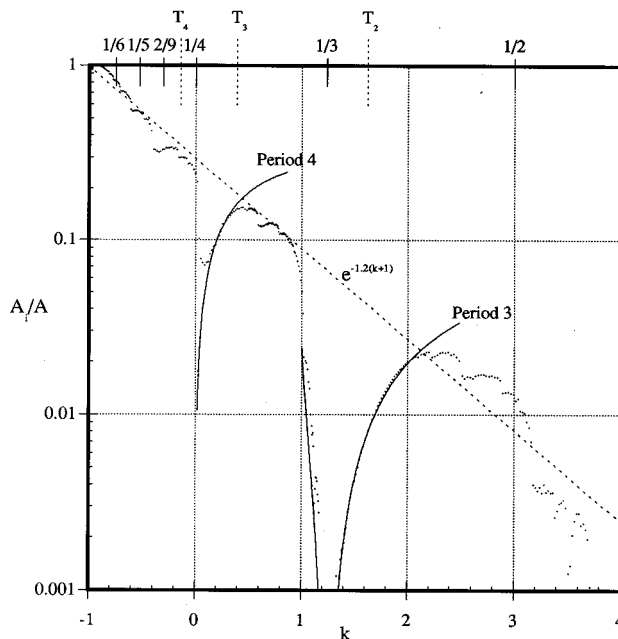
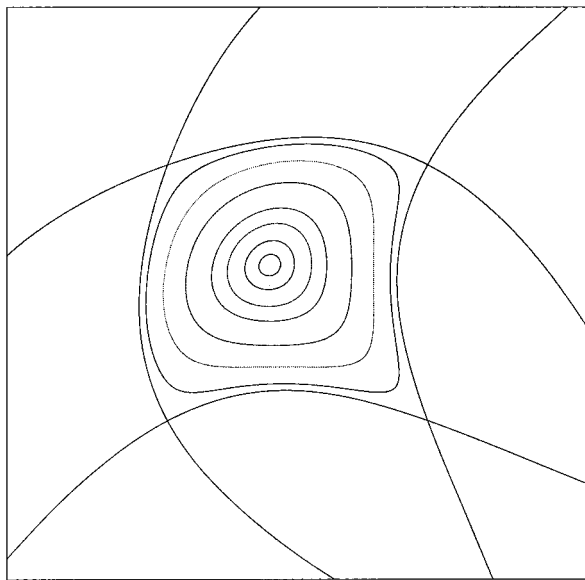


FIG. 9. Inaccessible fraction of the resonance zone for the Hénon map. The two solid curves represent simple approximations to the area enclosed by near heteroclinic connections for the period three and period four saddle orbits. The fraction falls off on average exponentially with k , aside from dips near prominent bifurcation points. Along the top are shown the k values for bifurcations of the elliptic point (labeled by rotation number p/q), and homoclinic bifurcations corresponding to the creation of type 2, 3, and 4 trellises.

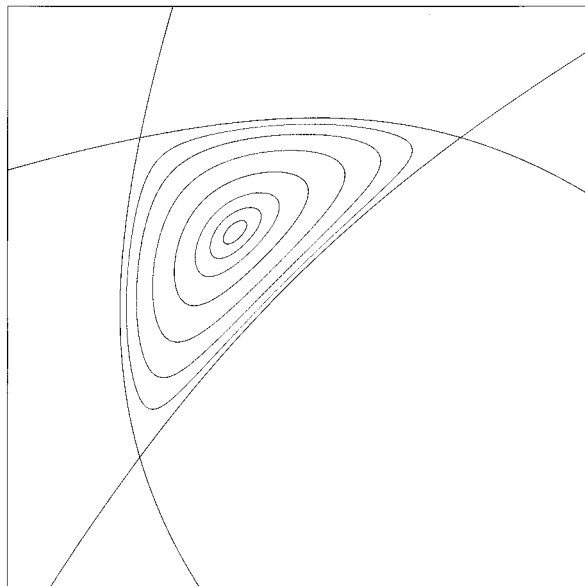
better in the next figure, which is the best representation of this information, Fig. 9. This shows the inaccessible fraction, $\mu(A_i)/\mu(A)$.

In Figure 9, the cutoff at a relative area of 10^{-3} is an artifact of our numerical method—it is quite difficult to reduce the error significantly. To do this one must increase the maximum number of iterations, t_{max} , to pick out narrow chaotic layers near invariant circles, and one must increase N to find all possible discontinuities in the exit time. It would be nice to improve the accuracy by detecting these discontinuities and find a form that fits $T(x)$ in their neighborhood, but we have not done that.

The most prominent features in Fig. 9 are local minima near $k=0$ and $k=1.25$. These correspond to the quadrupling and tripling bifurcations of the elliptic fixed point. In the period four case, a pair of orbits with rotation number $1/4$ are created at the bifurcation. Interestingly for $0 < k < 0.4$, the saddle period four orbit, which has points arranged on the square with corners $(\pm\sqrt{k}, \pm\sqrt{k})$, has nearly coincident stable and unstable manifolds—for practical purposes, a heteroclinic connection, Fig. 10. Furthermore for $0.2 < k < 0.4$ this feature dominates the inaccessible set. Using this approximation gives $\mu(A_i) \sim 4k$ for $k > 0$ —this formula, shown in Fig. 9, gives good agreement with the computed results. Of course, there are other inaccessible islands, most importantly islands around the elliptic $\omega=1/4$ orbit. These cause the fraction for $0 < k < 0.2$ to deviate from our simple form.



(a)



(b)

FIG. 10. Hénon map for $k=0.2$ and $k=1.6$. The outermost invariant curve surrounding the elliptic fixed point is closely approximated by a saddle connection of the $\omega=1/4$ and the $1/3$ saddle orbits, respectively. Bounds for the two figures are $(-1,1)\times(-1,1)$ and $(-1,0)\times(0,1)$, respectively.

A pair of period three orbits is created by saddle-node bifurcation at $k=1$. At $k=5/4$ the period three saddle collides with the elliptic fixed point and there are no encircling invariant curves. Near this bifurcation, the most important feature is the virtually perfect saddle connection of the manifolds of the period three saddle (see Fig. 10), which has points at $(-\beta, \beta) \rightarrow (-1+\beta, \beta) \rightarrow (-\beta, 1-\beta)$, with $\beta = \sqrt{k-1}$. Using a triangle as an approximation for this area gives $\mu(A_i) \sim 1/2(2\beta-1)^2$. The resulting curve is also shown in Fig. 9; it fits remarkably well for $1.28 < k < 2$. Note that, contrary to the impression given by Fig. 9, the inaccessible fraction does not go to zero at $k=1.25$. In particular, there is

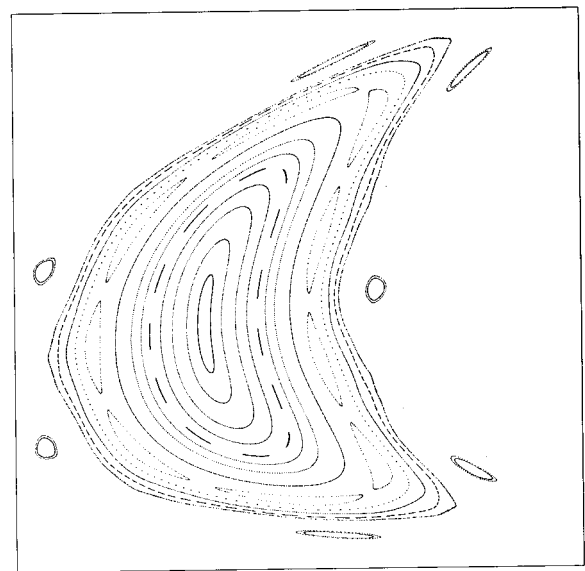


FIG. 11. One of the islands around a period three orbit at $k=1.25$, the period tripling point of the Hénon map. Plot bounds are $(-1.51, -0.597)\times(-1.48, -0.375)$.

a second period three orbit, $(1/2, -1/2) \rightarrow (-3/2, -1/2) \rightarrow (1/2, 3/2)$, that is elliptic. The island chain surrounding this orbit (see Fig. 11), has a relative area about 5×10^{-4} , accounting for most of the inaccessible area. There are no other visible islands.

There are other sharp drops in the inaccessible fraction, the most prominent occur at $k=-0.61, -0.414, 0.585, 0.78, 2.50$, and 3.17 . These occur when an invariant circle is destroyed, instantaneously opening up a new accessible region. The newly opened region will be ‘‘large’’ if the critical circle is just outside a large island chain. For example near $k=-0.4145$ there is a single invariant circle bounding $\omega=1/5$ island chain (in the range $6/31 < \omega < 7/36$). This invariant circle is destroyed by $k=-0.414$, leading to the opening of a new accessible domain, and consequent decrease in measure of the bounded orbits.

VII. CONCLUSIONS

We have shown that the average exit time from a region is given exactly by the ratio of the area of the accessible portion of the region to the area of the exit set in Eq. (11). It is interesting that this provides a justification for the oft used estimate that an ‘‘escape rate’’ from a region is given by the inverse of this ratio. We use Eq. (11) to provide a nice numerical tool for computing the measure of the bounded orbits for the Hénon map. Unfortunately, computational resources limit our accuracy in this calculation to a relative measure of about 10^{-3} .

For the future, it would be inviting to apply Eq. (11) to study the bounded orbits for higher dimensional maps, for example Moser’s canonical form for the quadratic symplectic map.²⁹ Such maps have important applications to particle accelerators.

ACKNOWLEDGMENTS

I would like to acknowledge the support of the National Science Foundation under Grant No. DMS-9305847, and support from a NATO Scientific Affairs Division Collaborative Research grant (No. 921181). This led to discussions with Robert MacKay, whose insights were central to this research.

- ¹C. F. F. K. Karney, A. B. Rechester, and R. B. White, "Effect of noise on the standard mapping," *Physica D* **4**, 425–438 (1982).
- ²R. S. MacKay, J. D. Meiss, and I. C. Percival, "Transport in Hamiltonian systems," *Physica D* **13**, 55–81 (1984).
- ³J. D. Hanson, J. R. Cary, and J. D. Meiss, "Algebraic decay in self-similar Markov chains," *J. Stat. Phys.* **39**, 327–345 (1985).
- ⁴A. J. Lichtenberg, M. A. Lieberman, and N. W. Murray, "The effect of quasi-accelerator modes on diffusion," *Physica D* **28**, 371–81 (1987).
- ⁵V. Rom-Kedar and S. Wiggins, "Transport in two-dimensional maps," *Arc. Rat. Mech. Anal.* **109**, 239–298 (1988).
- ⁶T. Horita, H. Hata, R. Ishizaki, and H. Mori, "Long-time correlations and expansion-rate spectra of chaos in Hamiltonian systems," *Prog. Theor. Phys.* **83**, 1065–1070 (1990).
- ⁷R. Ishizaki, H. Hata, T. Horita, and H. Mori, "Long-time correlations and anomalous diffusion due to accelerator modes in the standard maps," *Prog. Theor. Phys.* **84**, 179–184 (1990).
- ⁸R. Ishizaki, T. Horita, T. Kobayashi, and H. Mori, "Anomalous diffusion due to accelerator modes in the standard map," *Prog. Theor. Phys.* **85**, 1013–1022 (1991).
- ⁹R. W. Easton, "Transport through chaos," *Nonlinearity* **4**, 583–590 (1991).
- ¹⁰S. Wiggins, *Chaotic Transport in Dynamical Systems*, Interdisciplinary Applied Mathematics (Springer-Verlag, New York, 1991).
- ¹¹J. D. Meiss, "Symplectic maps, variational principles, and transport," *Rev. Mod. Phys.* **64**, 795–848 (1992).
- ¹²R. W. Easton, "Transport of phase space volume near isolated invariant sets," *J. Dyn. Diff. Eq.* **5**, 529–535 (1993).
- ¹³A. N. Yannacopoulos and G. Rowlands, "A model for the coexistence of diffusion and accelerator modes in a chaotic area-preserving map," *J. Phys. A* **26**, 6231–6249 (1993).
- ¹⁴R. W. Easton, J. D. Meiss, and S. Carver, "Exit times and transport for symplectic twist maps," *Chaos* **3**, 153–165 (1993).
- ¹⁵M. Kac, "On the notion of recurrence in discrete stochastic processes," *Bull. Am. Math. Soc.* **53**, 1002–1010 (1947).
- ¹⁶M. Kac, *Probability and Related Topics in Physical Sciences*, Lecture in Applied Mathematics, Proceedings for the Summer Seminar in Boulder, Colorado (Interscience, New York, 1957).
- ¹⁷M. Hénon, "Numerical study of quadratic area-preserving mappings," *Q. J. Appl. Math.* **27**, 291–312 (1969).
- ¹⁸S. R. Channon and J. L. Lebowitz, "Numerical experiments in stochasticity and heteroclinic oscillation," *Nonlinear Dynamics*, edited by R. H. G. Helleman (New York Academy of Science, New York, 1980), pp. 108–118.
- ¹⁹C. F. F. K. Karney, "Long time correlations in the stochastic regime," *Physica D* **8**, 360–380 (1983).
- ²⁰B. V. Chirikov and D. L. Shepelyansky, "Correlation properties of dynamical chaos in Hamiltonian systems," *Physica D* **13**, 395–400 (1984).
- ²¹Y. C. Lai, M. Ding, C. Grebogi, and R. Blümel, "Algebraic decay and fluctuations of the decay exponent in Hamiltonian systems," *Phys. Rev. A* **48**, 4661–4669 (1992).
- ²²N. Murray, "Critical function for the standard map," *Physica D* **52**, 220–245 (1991).
- ²³G. M. Zaslavsky, and M. K. Tippet, "Connection between recurrence-time statistics and anomalous transport," *Phys. Rev. Lett.* **67**, 3251–3254 (1991).
- ²⁴R. S. MacKay, "Transport in 3D volume-preserving flows," *J. Nonlinear Sci.* **4**, 329–354 (1994).
- ²⁵V. Rom-Kedar, A. Leonard, and S. Wiggins, "An analytical study of transport, mixing, and chaos in an unsteady vortical flow," *J. Fluid Mech.* **214**, 347–394 (1990).
- ²⁶V. Rom-Kedar, "Transport rates of a class of two-dimensional maps and flows," *Physica D* **43**, 229–268 (1990).
- ²⁷R. S. MacKay, J. D. Meiss, and I. C. Percival, "Resonances in area preserving maps," *Physica D* **27**, 1–20 (1987).
- ²⁸V. G. Gelfreich, V. F. Lazutkin, and M. B. Tabanov, "Exponentially small splittings in Hamiltonian systems," *Chaos* **1**, 137–142 (1991).
- ²⁹J. K. Moser, "On quadratic symplectic mappings," *Math. Z.* **216**, 417–430 (1994).